Kinetic Analysis of the Imidization of Poly(styrene-*co*-maleic anhydride) with Aniline in the Melt

He-Yang Liu,[1,2] Zhen Yao,[1] Kun Cao,[1] Bo-Geng Li[1]

[1]*State Key Laboratory of Chemical Engineering, Institute of Polymerization and Polymer Engineering, Department of Chemical and Biological Engineering, Zhejiang University, Hangzhou 310027, China*
[2]*School of Biological and Chemical Engineering, Zhejiang University of Science and Technology, Hangzhou 310023, China*

Received 22 October 2008; accepted 15 November 2009
DOI 10.1002/app.31800
Published online 4 February 2010 in Wiley InterScience (www.interscience.wiley.com).

ABSTRACT: On the basis of the competitive reactions of intermediate poly(styrene-*co*-*N*-phenyl maleamic acid) (SNPMA) to produce either poly(styrene-*co*-maleic anhydride) (SMA) or poly(styrene-*co*-*N*-phenyl maleimide) (SNPMI), the imidization kinetics of SMA with aniline in the molten state were investigated by a novel approach. The volatiles emitted during the reaction of SNPMA were monitored online with both thermogravimetric analysis and Fourier transform infrared (FTIR) integrated technology. The experimental results directly and definitely indicate that the amidization reaction from SMA to SNPMA in the melt was reversible. Moreover, the kinetic parameters of the competitive reactions of SNPMA in the melt to produce either SMA or SNPMI were determined by FTIR analysis and then compared with those parameters in solution that were obtained in our previous study. It was also implied that the forward ring-opening reaction of SMA in the melt was nearly instantaneous and that the rates of the competitive reactions of SNPMA to produce either SMA or SNPMI were crucial for the total imidization of SMA. © 2010 Wiley Periodicals, Inc. J Appl Polym Sci 116: 2951–2957, 2010

Key words: kinetics (polym.); reactive extrusion

INTRODUCTION

In recent decades, chemically modified reactions based on polymers have been widely used to broaden the application windows of polymers. These reactions can be performed in solution, in which the use of a solvent allows good control of the reaction temperature, medium viscosity, and reactivity between polymers and relative selected reactants. However, there are many more advantages when these reactions are carried out in the melt.[1–3] For example, a lack of solvent leads to no need for the precipitation of products or the removal of the solvent. The reaction rates in polymer melts are much higher than those in solution because of the higher reactant concentration and reaction temperatures. Moreover, the reactions may be combined with the polymer processing procedure simultaneously to develop a reactive processing technology, which is very promising because of its rapidity, flexibility, ecology, low cost, and so on.[1–8] Applications of chemical reactions in polymer melts are widely practiced and include the alcoholysis of ethylene vinyl acetate copolymers,[9,10] the chlorination of isobutene–diene rubber,[11,12] the functional grafting and crosslinking of polymers,[13–16] and the imidization of the polymers containing anhydride groups with primary amines.[17–26]

Poly(styrene-*co*-*N*-substituted maleimide) (SMI) has excellent properties, including good heat resistance and adjustable compatibility when it is blended with styrenic polymers and polar polymers.[27–29] SMI can be effectively and flexibly prepared by the direct imidization of poly(styrene-*co*-maleic anhydride) (SMA) with primary amines, on which plenty of work has been focused.[27–35] Moreover, the continuous imidization of SMA in the melt through reactive extrusion should be of great interest to industry.

Schmidt-Naake and coworkers[20,21] showed that the reactivity was remarkably influenced by the imidization reagent itself, which was consistent with other studies.[36] Specifically, the imidization conversion reached 80% after 5 min in an extruder when the molar ratio of aniline (ANL) to anhydride was about 1.[22] The conversion reached almost 100% when ANL was substituted by octodecylamine.[23] However, another experiment showed that the conversion could not be higher than 80%, even the molar ratio of ammonia to anhydride exceeded 5

Correspondence to: Z. Yao (yaozhen@zju.edu.cn) or K. Cao (kcao@che.zju.edu.cn).

Contract grant sponsor: National Natural Science Foundation of China; contract grant numbers: 50390097, 50773069, and 50873090.

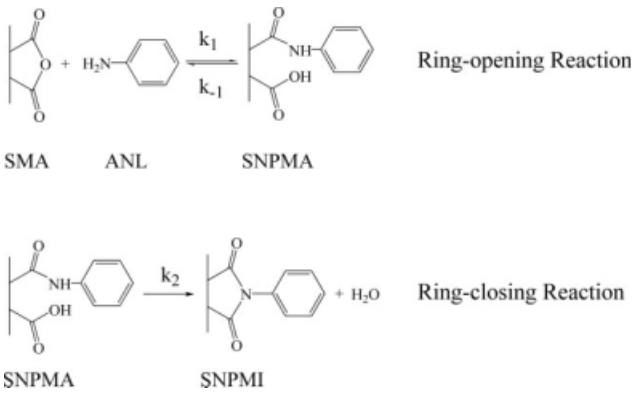

Scheme 1 Imidization mechanism of SMA with ANL.

when reacted at 240–265°C in a twin-screw extruder with a mean residence time of 2 min.[24] When naphthylamine was used as the imidization reagent and the molar ratio of naphthylamine to anhydride was about 0.6, the imidization conversion just reached 25% in the first part of the twin-screw extruder (mean residence time = 38 s) at 200°C and was hardly changed after that.[25] However, because they were restricted by the experimental approach or apparatus, especially by the volatization of the imidization reagent and sampling technique, the results were just semiquantitative, even qualitative. A quantitative study on this reaction is absent, and the understanding of this reaction is still poor.

In our previous article,[37] we already discussed the imidization of SMA with ANL in solution. As shown in Scheme 1, the imidization mechanism can be considered as two consecutive reactions: a reversible ring opening to produce poly(styrene-*co*-*N*-phenyl maleamic acid) (SNPMA) and an irreversible intrachain ring closing to form the corresponding poly(styrene-*co*-*N*-phenyl maleimide) (SNPMI). The kinetic parameters in solution were obtained. Furthermore, it should be very interesting to determine whether the imidization of SMA in the melt can be widened.

In this study, the imidization of SMA in the melt was investigated in a novel approach with intermediate SNPMA as the starting reactant. The volatiles emitted during the reaction of SNPMA were monitored online and analyzed with thermogravimetric analysis (TGA)/Fourier transform infrared (FTIR) coupling technology. Furthermore, the kinetic parameters of the imidization of SMA in the melt are discussed and compared with those in solution.

EXPERIMENTAL

Materials

ANL, tetrahydrofuran (THF), and hexane were all analytical reagent grade and were used as received. A random SMA with 16 wt % maleic anhydride (MAh) was synthesized in our laboratory.[38,39]

Preparation of SNPMA

The reaction was carried out under nitrogen in a jacketed reactor with an anchor agitator. The reaction temperature was controlled at 20 ± 0.5°C. A given amount of SMA was charged to the reactor, followed by the addition of THF and intensive agitation. After a homogeneous solution of 10 wt % SMA was obtained, a specified amount of ANL (molar ratio of ANL to anhydride = 3) was added to the reactor, and the reaction started to proceed. It was calculated that SMA was almost totally converted to SNPMA after 24 h under these conditions, according to the kinetics reported in our previous article.[37] The mixture was dropped into a 10-fold excess of hexane after 30 h. The crude product was alternately dissolved with THF and precipitated with hexane three times. Finally, the purified product was dried *in vacuo* at 50°C for 24 h.

Reaction of SNPMA in the melt

A set of batch reactions of SNPMA in the melt were isothermally carried out at 190, 200, and 210°C in a TGA system (PerkinElmer Pyris 1 TGA, Waltham, MA) under nitrogen until the weight of the samples did not change. The composition of the residuals was analyzed. Another set of batch reactions were performed to analyze the volatiles in an integrated TGA–FTIR online system (Mettler–Toledo TGA/SDTA851e, Schwerzenbach, Switzerland and Thermo Nicolet 5700 FTIR integrated system, Waltham, MA) under nitrogen with a scanning range of 50–550°C and a scanning rate of 20°C/min.

Sample composition analysis

The chemical compositions of the samples before and after isothermal reaction in the TGA system were analyzed by FTIR with a Thermo Nicolet 5700 FTIR spectrometer. The samples for FTIR analysis were prepared by grinding with KBr and then pressing into a film. We calculated the compositions of the obtained products from the reduced absorbance at 1545 cm^{-1} and the increased absorbance at 1380 cm^{-1} by choosing the absorbance at 2926 cm^{-1} ($—CH_2$) as an internal reference.

RESULTS AND DISCUSSION

FTIR characterization of the samples

The typical FTIR spectra of SNPMA before and after reaction through isothermal TGA are shown in Figure 1. The absorbances at 1860 (C—O—C) and

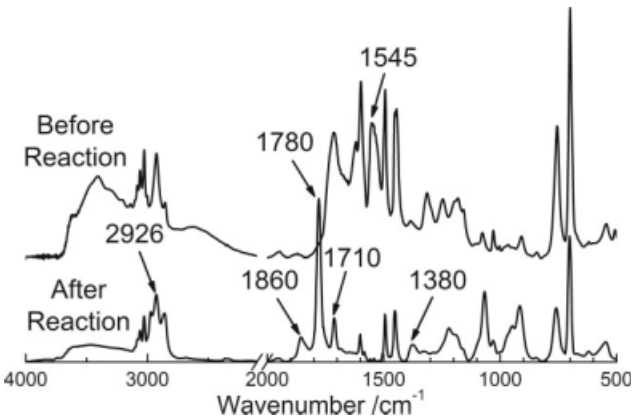

Figure 1 Typical FTIR spectra of SNPMA before and after the reaction through isothermal analysis.

1780 cm^{-1} (C═O) characterized the SMA component, the absorbances at 1710 (O═C—N) and 1545 cm^{-1} (C—NH—) characterized the SNPMA component, and the absorbances at 1780 (C═O), 1710 (O═C—N), and 1380 cm^{-1} (C—N—C) characterized SNPMI. Because the amount of $-CH_2$ did not change during the reaction, the absorbance at 2926 cm^{-1} ($-CH_2$) was chosen as the inner standard. The composition of the obtained products was calculated from the reduced absorbance at 1545 cm^{-1} and the increased absorbance at 1380 cm^{-1}. The calibration curves used in the calculation are shown in Figure 2. The standard samples used for calibration were acquired by the mixture of SNPMA or SNPMI with SMA in a series of molar ratios.

Reaction mechanism

In our previous study,[37] we assumed that the ring-opening (amidization) reaction of SMA to produce

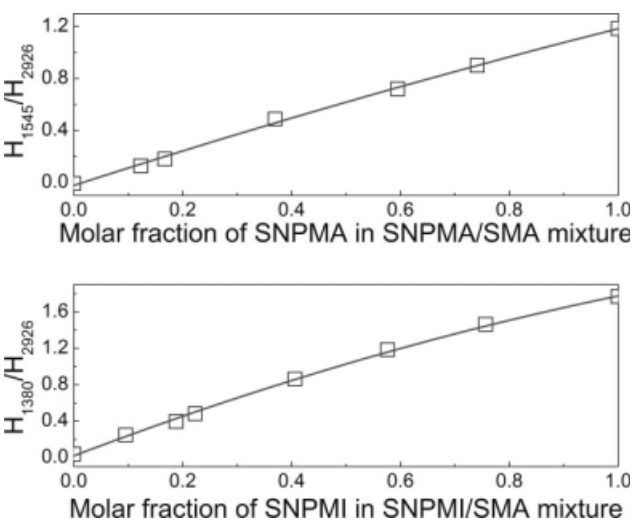

Figure 2 Calibration curves of the FTIR analysis. H_{1545}, H_{1380}, and H_{2926} are the height of the absorbance peak at 1545, 1380, and 2926 cm^{-1}, respectively.

TABLE I
Equilibrium Constants of the Ring-Opening Reaction of SMA with ANL in Solution

Temperature (°C)	$k_1^{solution}$ (L mol^{-1} s^{-1})	$k_{-1}^{solution}$ (s^{-1})	$k_1^{solution}/k_{-1}^{solution}$ (L/mol)
0	7.2×10^{-2}	1.7×10^{-7}	4.3×10^{5}
50	4.6×10^{-1}	1.1×10^{-5}	4.2×10^{4}
100	1.8	2.3×10^{-4}	7.8×10^{3}
150	5.0	2.3×10^{-3}	2.2×10^{3}
200	1.1×10^{1}	1.4×10^{-2}	7.8×10^{2}

All the data listed in this table were calculated as follows:

$k_1^{solution} = 1.10 \times 10^4\, e^{-27{,}100/RT}$ ($1 \cdot mol^{-1} \cdot s^{-1}$)

$k_{-1}^{solution} = 7.82 \times 10^4\, e^{-61{,}000/RT}$ (s^{-1})

These equations were obtained from a previous article.[37]

SNPMA was reversible, as according to the literature.[36,40] However, with regard to the amidization of SMA, there different opinions still exist. For instance, Wolske's study[41] on the SMA/benzylamine system in dimethylformamide solution showed that the ring-opening reaction of SMA was an irreversible reaction. On the basis of the kinetic parameters we obtained in the previous study, it is clearly shown in Table I that the reverse reaction of the ring-opening reaction of SMA in the solution was actually very slow, and the equilibrium constant was actually very large, even when the reaction temperature was up to 150°C. In other words, the reversibility can be ignored when the ring-opening reaction of SMA is conducted in solution in such a moderate temperature range. However, when the imidization of SMA is performed in the melt, for example, through reactive extrusion, the situation is different. First, the higher reaction temperature leads to a decreased equilibrium constant. Second, the evaporation of the ANL cannot be ignored because the process temperature is usually higher than the boiling point of ANL. Then, the reverse reaction should be more significant if it does exist. Therefore, it was crucial to demonstrate whether the amidization of SMA with ANL in the melt was a reversible reaction.

Figure 3 shows the thermal decomposition curves and their derivative curves of SMA, SNPMA, and SNPMI, respectively. SMA lost 94% of its original weight at 300–450°C, and SNPMI lost 98% of its original weight at 350–480°C. On the other hand, SNPMA experienced two weight losses; one was about a 14% loss of its original weight at 120–210°C, which was similar with the glass-transition temperature (T_g) range of SNPMA (T_g = 154°C, ΔT_g = 40°C, starting T_g = 128°C, ending T_g = 170°C),[42] and the other was about a 91% loss of the residual weight at 330–450°C, which was similar to the weight loss of SMA. Therefore, the first weight loss of SNPMA

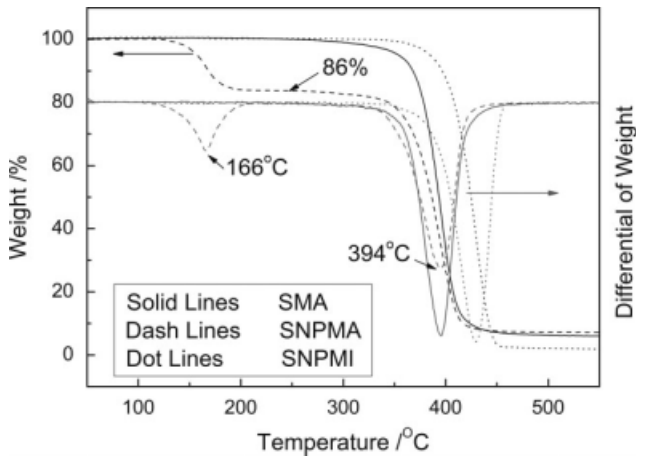

Figure 3 TGA curves and their derivative curves for SMA, SNPMA, and SNPMI.

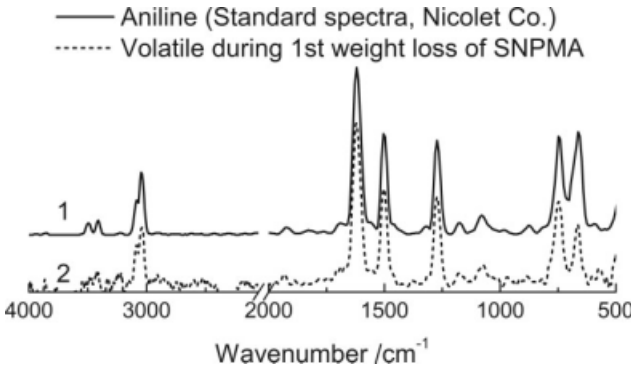

Figure 4 FTIR spectra of the volatiles during the first weight loss of SNPMA (at 166°C) and ANL.

should have been caused by the reverse ring-opening reaction of SMA rather than the forward ring-closing reaction of SNPMA.

To reveal the thermal reaction mechanism of SNPMA, online TGA–FTIR integrated technology was adopted to analyze the gas phase during the thermal decomposition process. The FTIR spectra of the gas phase at various times during the thermal decomposition process of SNPMA are shown in Figures 4 and 5. The spectrum of the volatiles generated during the first weight loss of SNPMA (Fig. 4) matched well the standard spectrum of ANL. Furthermore, the spectrum of the volatiles generated during the second weight loss (Fig. 5) was similar to the spectrum of the volatiles generated during the weight loss of SMA. Therefore, we concluded that the ring-opening reaction in the melt from SMA to SNPMA was reversible.

Kinetic equations

The entire temperature range of the isothermal reaction of SNPMA in this study was higher than the boiling temperature of ANL. We assumed that the ANL generated in the reaction was removed immediately and completely under nitrogen. In other words, the concentration of ANL was near zero in this reaction system. Therefore, a pair of competitive reactions of *N*-phenyl maleamic acid (NPMA) groups on the SNPMA chain to produce either MAh groups or *N*-phenyl maleimide (NPMI) groups existed during the isothermal process, and the kinetic equations could be written as follows:

$$\frac{d[\mathrm{MAh}]_t}{dt} = k_{-1}^{\mathrm{melt}}[\mathrm{NPMA}]_t \tag{1}$$

$$\frac{d[\mathrm{NPMA}]_t}{dt} = -(k_{-1}^{\mathrm{melt}} + k_2^{\mathrm{melt}})[\mathrm{NPMA}]_t \tag{2}$$

$$\frac{d[\mathrm{NPMI}]_t}{dt} = k_2^{\mathrm{melt}}[\mathrm{NPMA}]_t \tag{3}$$

where $[\mathrm{MAh}]_t$, $[\mathrm{NPMA}]_t$, and $[\mathrm{NPMI}]_t$ are the molar concentrations of the MAh groups, NPMA groups, and NPMI groups, respectively, at t minutes.

The reduced weight of the polymer at t minutes [W_t (%)] could be expressed as follows:

$$W_t(\%) = \frac{M_{\mathrm{MAh}}[\mathrm{MAh}]_t + M_{\mathrm{NPMA}}[\mathrm{NPMA}]_t + M_{\mathrm{NPMI}}[\mathrm{NPMI}]_t + M_{\mathrm{St}}[\mathrm{St}]_t}{M_{\mathrm{NPMA}}[\mathrm{NPMA}]_0 + M_{\mathrm{St}}[\mathrm{St}]_0} \tag{4}$$

where M_{MAh}, M_{NPMA}, M_{NPMI}, and M_{St} are the molecular weights of the MAh groups, NPMA groups, NPMI groups, and styrene (St) groups, respectively; $[\mathrm{NPMA}]_0$ and $[\mathrm{St}]_0$ are the initial molar concentrations of the NPMA groups and St groups, respectively; and $[\mathrm{St}]_t$ is the molar concentration of the St groups at t minutes, which is obviously equal to $[\mathrm{St}]_0$. Therefore

$$\frac{1 - W_t(\%)}{1 - W_\infty(\%)} = \frac{M_{\mathrm{NPMA}} - M_{\mathrm{MAh}}x_{\mathrm{MAh},t} - M_{\mathrm{NPMA}}x_{\mathrm{NPMA},t} - M_{\mathrm{NPMI}}x_{\mathrm{NPMI},t}}{M_{\mathrm{NPMA}} - M_{\mathrm{MAh}}x_{\mathrm{MAh},\infty} - M_{\mathrm{NPMA}}x_{\mathrm{NPMA},\infty} - M_{\mathrm{NPMI}}x_{\mathrm{NPMI},\infty}} \tag{5}$$

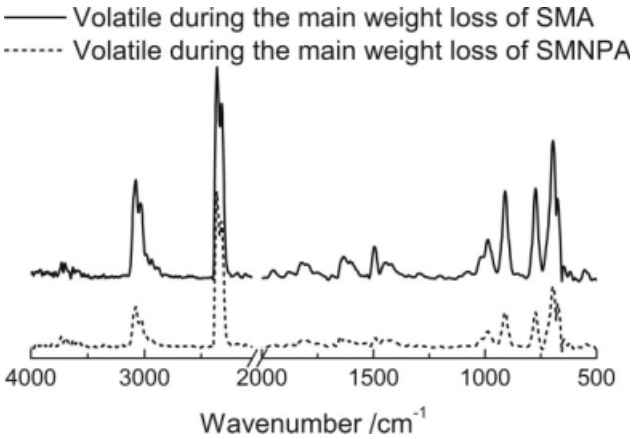

Figure 5 FTIR spectra of the volatiles for SMA and SNPMA during the main weight loss (at 394°C).

where W_∞ (%) is the final weight of the polymer; $x_{MAh,t}$, $x_{NPMA,t}$, and $x_{NPMI,t}$ are the molar fractions of the MAh groups, NPMA groups, and NPMI groups, respectively, in the previous three groups at t minutes; and $x_{MAh,\infty}$, $x_{NPMA,\infty}$, and $x_{NPMI,\infty}$ are the final molar fractions of the MAh groups, NPMA groups, and NPMI groups, respectively, in the previous three groups. Because the overall molar amount of MAh groups, NPMA groups, and NPMI groups during the reaction should be constant, they could be obtained as follows:

$$x_{MAh,t} + x_{NPMA,t} + x_{NPMI,t} = x_{MAh,\infty} + x_{NPMA,\infty} + x_{NPMI,\infty} = 1 \quad (6)$$

$$\frac{x_{MAh,t}}{x_{NPMI,t}} = \frac{x_{MAh,\infty}}{x_{NPMI,\infty}} = \frac{k_{-1}^{melt}}{k_2^{melt}} = \text{Constant} \quad (7)$$

Therefore, the molar composition of the polymer at t minutes can be calculated from the final composition of the resulting polymer through the combination of eqs. (5)–(7). Then, the kinetic parameters can be estimated.

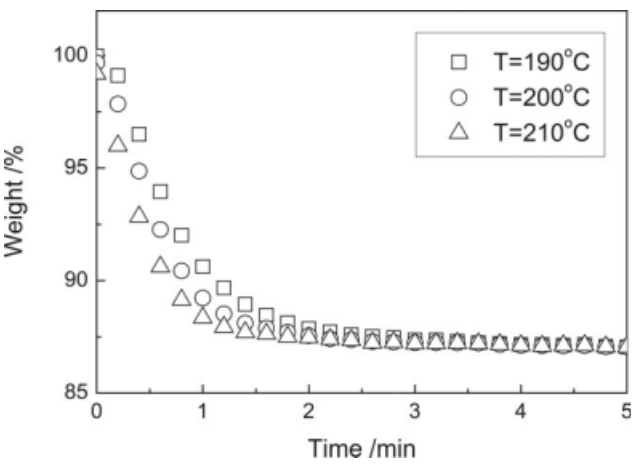

Figure 6 Sample weight versus the reaction time at different temperatures.

TABLE II
Compositions of the Residue of SNPMA After Isothermal TGA

Temperature (°C)	SNPMA	SNPMI	SMA
190	0	0.112	0.888
200	0	0.109	0.891
210	0	0.097	0.903

Kinetic parameters

Figure 6 shows the isothermal scanning curves of SNPMA at different temperatures. The reaction rate was so fast that the reaction was almost completed in 5 min. The molar compositions of the final products are listed in Table II. Because the molar fraction of NPMI was much lower than that of MAh, we concluded that the rates of the pair of competitive reactions were very different in the temperature range adopted in this study.

With the approach mentioned previously, the molar composition at different reaction times was obtained, as shown in Figure 7. The kinetic parameters were estimated and are listed in Table III. Compared with the kinetic parameters in solution, the pre-exponential factor of the kinetic parameters in the melt seemed to be slightly higher; this was similar to the results reported by Dickinson and Sung[40] for the thermal imidization of poly(amic acid). This could be attributed to the increased collision probability due to the higher concentration of reaction groups. Moreover, it is also shown in Table III that the activity energy of the kinetic parameters was

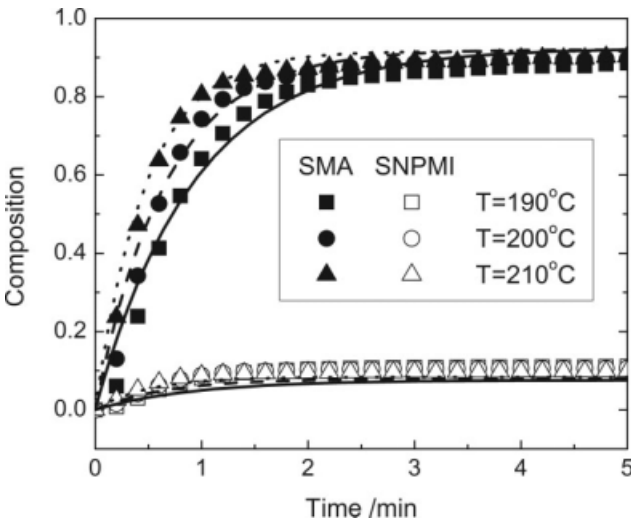

Figure 7 Composition versus the reaction time for various temperatures. The points represent experimental data; the lines show simulation results.

close either in solution or in the melt; this was similar to the results reported by Hu et al.[43] Therefore, it was implied that the significantly increased viscosity did not bring a great restriction of the motion of the reaction groups on the polymer chains because the competitive reactions mentioned previously were the intramolecular reactions.

On the bases of the reaction mechanism and the experimental results, the kinetic parameters of the reverse ring-opening reaction of SMA and the forward ring-closing reaction of SNPMA were obtained. However, the kinetic parameter of the forward ring-opening reaction of SMA, which was also very indispensable for the understanding of the imidization of SMA, was still absent. To investigate the effect of the kinetic parameter of the forward ring-opening reaction of SMA on the imidization of SMA in the molten state, the molar composition during the imidization of SMA was calculated. In this simulation, the reverse rate of the ring-opening reaction of SMA and the forward rate of the ring-closing reaction of SNPMA were calculated according to the parameters for the melt reaction (Table III), whereas the forward rate of the ring-opening reaction of SMA was assumed in a range from the value of the forward rate of the ring-opening reaction of SMA in solution to 100 times that value. The assumption should have been reasonable according to the study of Dickinson and Sung,[40] who indicated that the reaction between amines and anhydride was faster in film than in solution because the amine was restricted to a smaller space and the frequency of the collision between amine and anhydride was increased with the cage effect. The relationship of the composition with the reaction time for various conditions is plotted in Figure 8. The simulation results indicate that the forward rate of the ring-opening reaction of SMA had little influence on the imidization process in the melt. In other words, the forward ring-opening reaction of SMA in the melt should have been nearly instantaneous. The rates of the competitive reactions of SNPMA to produce either SMA or SNPMI should have been crucial for the imidization of SMA. Meanwhile, it was reasonable to use the kinetic parameter of the forward ring-opening in solution as that in the melt.

TABLE III
Kinetic Rate Constants of the Competitive Reactions of SNPMA in Solution and in the Melt

	k_{-1} (s^{-1})	k_2 (s^{-1})
In solution[a]	$7.82 \times 10^4\ e^{-61,000/RT}$	$9.49 \times 10^4\ e^{-65,800/RT}$
In the melt	$1.02 \times 10^5\ e^{-60,200/RT}$	$1.12 \times 10^5\ e^{-70,200/RT}$

[a] The data were taken from ref. 37.

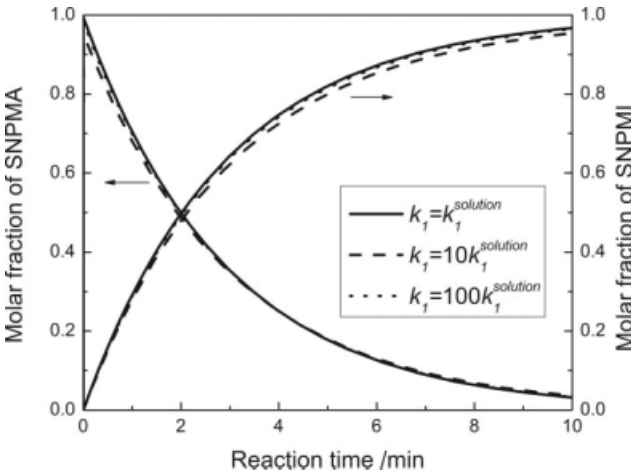

Figure 8 Prediction of the imidization of SMA under melt conditions for various values of k_1 [$k_{-1} = k_{-1}^{melt} = 1.02 \times 10^5\ e^{-60,200/RT}$ (s^{-1}), $k_2 = k_2^{melt} = 1.12 \times 10^5\ e^{-70,200/RT}$ (s^{-1}), ANL/MAh = 1, temperature = 230°C].

CONCLUSIONS

We investigated the competitive reactions of SNPMA to produce either SMA or SNPMI by using TGA–FTIR integrated technology. The experimental results indicate that the amidization reaction from SMA to SNPMA in the melt was reversible. The kinetic parameters of the competitive reactions of SNPMA to produce either SMA or SNPMI were determined in the melt, which could be expressed as follows:

$$k_{-1}^{melt} = 1.02 \times 10^5 e^{-60,200/RT}(1/s)$$
$$k_2^{melt} = 1.12 \times 10^5 e^{-70,200/RT}(1/s)$$

where T is the reaction temperature and R is the universal gas constant. When compared with those parameters in the solution reaction, we found that: (1) the pre-exponential factor in the melt was higher than that in solution, and (2) the activity energy in the melt was close to that in solution. The higher pre-exponential factor was attributed to the increased collision probability due to the higher concentration of reaction groups. The similar activity energy implied that the significantly increased viscosity did not lead to a great restriction of the motion of the reaction groups on the polymer chains because the competitive reactions mentioned previously were intramolecular reactions. Furthermore, it was also shown that the forward ring-opening reaction of SMA in the melt was nearly instantaneous, and the rates of the competitive reactions of SNPMA to produce either SMA or SNPMI should have been crucial for the imidization of SMA. Meanwhile, it was reasonable to use the kinetic parameter of the

forward ring-opening reaction of SMA in solution as that in the melt.

The authors are indebted to Guo-Hua Hu from France for helpful discussions.

References

1. Xanthos, M. Reactive Extrusion: Principles and Practises; Hanser: Munich, 1992.
2. Tzoganakis, C. Adv Polym Technol 1989, 9, 321.
3. Lambla, M. Macromol Symp 1994, 83, 37.
4. Cassagnau, P.; Bounor-Legare, V.; Fenouillot, F. Int Polym Proc 2007, 22, 218.
5. Sneller, J. A. Mod Plast Int 1985, 15, 42.
6. Kroschwitz, J. I.; Mark, H. F.; Bikales, N.; Overberger, C. G.; Menges, G. Encyclopedia of Polymer Science and Engineering; Wiley: New York, 1988; p 101.
7. Lambla, M. Chem Eng Technol 1991, 63, 1137.
8. Lambla, M. Polym Proc Eng 1987, 5, 295.
9. Bouilloux, A.; Druz, J.; Lambla, M. Polym Eng Sci 1987, 27, 1221.
10. Hu, G. H.; Lindt, J. T.; Lambla, M. J Appl Polym Sci 1992, 46, 1039.
11. Kowalski, R. C.; Davis, W. M. U.S. Pat. 4,508,592 (1985).
12. Kowalski, R. C. Chem Eng Prog 1989, 85, 67.
13. Shi, Q.; Zhu, L. C.; Cai, C. L.; Yin, J. H.; Costa, G. J Appl Polym Sci 2006, 101, 4301.
14. Badrossamay, M. R.; Sun, G. Polym Eng Sci 2009, 49, 359.
15. Passaglia, E.; Coiai, S.; Augier, S. Prog Polym Sci 2009, 34, 911.
16. Badel, T.; Beyou, E.; Bounor-Legare, V.; Chaumont, P.; Flat, J. J.; Michel, A. J Polym Sci Part A: Polym Chem 2007, 45, 5215.
17. Song, Z.; Baker, W. E. J Polym Sci Part A: Polym Chem 1992, 30, 1589.
18. Lu, Q. W.; Macosko, C. W.; Horrion, J. J Polym Sci Part A: Polym Chem 2005, 43, 4217.
19. Hu, G. H.; Holl, Y.; Lambla, M. J Polym Sci Part A: Polym Chem 1992, 30, 625.
20. Schmidt-Naake, G.; Klak, M. Chem Eng Technol 2000, 23, 772.
21. Schmidt-Naake, G.; Becker, H. G.; Klak, M. Macromol Symp 2001, 163, 213.
22. Koch, O.; Waniczek, H. Ger. Pat. 3,430,802 (1986).
23. Bourland, L. G.; London, M. E.; Cooper, T. A. Seminar on Reactive Processing; Rapra: Shawbury, England, 1989.
24. Vermeesch, I.; Groeninckx, G. J Appl Polym Sci 1994, 53, 1365.
25. Machado, A. V.; Covas, J. A.; van Duin, M. J Appl Polym Sci 1999, 71, 135.
26. Vazquez-Rodriguez, S.; Sanchez-Valdes, S.; Rodriguez-Gonzalez, F. J.; Gonzalez-Cantu, M. C. Macromol Mater Eng 2007, 292, 1012.
27. Seo, Y.; Kim, H. J.; Kim, Y. J.; Rhee, H. W. Polym Eng Sci 2002, 42, 951.
28. Lim, J. C.; Cho, K. Y.; Park, J. K. J Appl Polym Sci 2008, 108, 3632.
29. Yuan, Y.; Siegmann, A.; Narkis, M.; Bell, J. P. J Appl Polym Sci 1996, 61, 1049.
30. Moore, E.; Pickelman, D. U.S. Pat. 3,801,549 (1974).
31. DiGiulio, A. V. U.S. Pat. 3,998,907 (1976).
32. Otani, I.; Sato, Y.; Watanabe, A. Jpn. Pat. 58–180506 (1983).
33. Nakagawa, K.; Tanaka, M.; Kishimoto, A. Jpn. Pat. 58–217522 (1983).
34. Tsumura, R.; Ikeda, K.; Muraishi, T.; Wang, J. K. Eur. Pat. 0,403,240 (1990).
35. van Den Berg, H. J.; Maassen, M. H. G.; Steenbakkers, L. W. WIPO Pat. 9,945,039 (1999).
36. Hu, G. H.; Lindt, J. T. Polym Bull 1992, 29, 357.
37. Liu, H. Y.; Cao, K.; Huang, Y.; Yao, Z.; Li, B. G.; Hu, G. H. J Appl Polym Sci 2006, 100, 2744.
38. Yao, Z.; Li, B. G.; Cao, K.; Pan, Z. R. J Appl Polym Sci 1998, 67, 1905.
39. Yao, Z.; Li, B. G.; Wang, W. J.; Pan, Z. R. J Appl Polym Sci 1999, 73, 615.
40. Dickinson, P. R.; Sung, C. S. P. Macromolecules 1992, 25, 3758.
41. Wolske, K. A. Ph.D. Dissertation, University of Minnesota, 1996; p 66.
42. Liu, H. Y.; Cao, K.; Yao, Z.; Li, B. G.; Hu, G. H. J Appl Polym Sci 2007, 104, 2418.
43. Hu, G. H.; Flat, J. J.; Lambla, M. Makromol Chem Macromol Symp 1993, 79, 137.